TNF-a activates at least two apoptotic signaling cascades

Carole Sidoti-de Fraisse, Vincent Rincheval, Yanick Risler, Bernard Mignotte, Jean-Luc Vayssière

Oncogene (1998) 17, 1639–1651

http://www.stockton-press.co.uk/onc

TNF-α activates at least two apoptotic signaling cascades

Carole Sidoti-de Fraisse, Vincent Rincheval, Yanick Risler, Bernard Mignotte and Jean-Luc Vayssière

Centre de Génétique Moléculaire, Centre National de la Recherche Scientifique, F-91198 Gif-sur-Yvette cedex, and Université de Versailles-St Quentin-en-Yvelines, 45 avenue des Etats-Unis, F-78035 Versailles cedex France

Apoptosis, the process whereby cells activate an intrinsic death program, can be induced in HeLa cells by TNF-α treatment. The aims of the present study were (i) to examine the precise role and the origin of Reactive Oxygen Species (ROS) in the TNF-α-induced programmed cell death, (ii) to characterize and order the morphological and mitochondrial changes associated with this process and (iii) to link these events with the activation of caspases. Analyses were performed on TNF-α-treated cells in the presence of an anti-oxidant, or of a general caspase inhibitor. To assess the role of mitochondria in the cell death signal transduction, these studies were also realized on HeLa-variant cell lines lacking functional mitochondrial respiratory chain. We show that at least two separate signaling cascades, both mediated by Z-VAD-sensitive caspase(s), contribute to the TNF-α-induced apoptosis of HeLa cells. One signaling pathway involves an early mitochondria-dependent ROS production, the other being ROS-independent.

Keywords: apoptosis; caspase; mitochondria; ROS

Introduction

Programmed cell death (PCD), also known as apoptosis, the process whereby cells activate an intrinsic death program, is a critical element in the repertoire of potential cellular responses, as are cell differentiation or proliferation. All nucleated mammalian cells, both in developing and mature organs, are able to undergo PCD and constitutively express all the protein components required to execute the death program, which are normally suppressed by extracellular survival signals. Moreover, it seems that new macromolecular synthesis, when necessary for PCD, contributes to the activation rather than to the execution of the death program (Raff, 1992; Weil *et al*., 1996).

The programmed cell death cascade can be conveniently divided into several phases. During the activation phase, multiple signaling pathways, initiated by the various death-triggering signals, lead to the central control of the cell death machinery and activate it. This is followed by the execution stage, in which the activated machinery acts on multiple cellular targets, and, finally, the destruction phase in which the dead or dying cell is broken down.

A most important clue to the molecular nature of the death program came initially from genetic studies in *C. elegans* that led to the identification of a dozen cell death genes (*ced*) that are responsible for one aspect or another of cell death processes (Ellis *et al*., 1991). Three of these genes stand out. Two of them, *ced-3* and *ced-4* are required to execute the cell death program. The third one, *ced-9*, antagonizes the death activities of *ced-3* and *ced-4*. Moreover, genetically, *ced-4* has been placed between *ced-9* and *ced-3* in the pathway leading to cell death (Shaham and Horvitz, 1996). Spectacular progress arose with their cloning, when it became clear that they encoded components of a universal and highly conserved death machinery. CED-3 protein turned out to be a member of a family of cysteine proteases, known as caspases (Yuan *et al*., 1993). The mammalian caspase family now comprises at least ten known members, most of which have been definitively implicated in PCD (Duan *et al*., 1996; Fraser and Evan, 1996; McCarthy *et al*., 1997). Caspases mediate PCD by cleaving selected intracellular proteins, including proteins of the nucleus, nuclear lamina, cytoskeleton, endoplasmic reticulum and cytosol.

CED-9 protein is homologous to a family of many members termed the Bcl-2 family (Reed, 1997). Some members, such as Bcl-2 or BCl-x_L, inhibit PCD, whereas others, such as Bax and Bik, promote cell death. The various family members (referred to here as Bcl-2s), which are primarily localized to intracellular membranes, can dimerize with one another, with one monomer antagonizing or enhancing the function of the other (Korsmeyer, 1995). Recent reports have shown that, in both worm and mammalian cells, the anti-apoptotic Bcl-2s act upstream of the 'execution caspases' somehow preventing their proteolytic processing into active killers (Shaham and Horvitz, 1996; Golstein, 1997). Two main mechanisms of action have been proposed to connect Bcl-2s to caspases. In the first one, anti-apoptotic Bcl-2s would maintain cell survival by dragging CED-4 or CED-4 like/caspase complexes to intracellular membranes, keeping them in an inactive conformation and in this way preventing their activation (Chinnaiyan *et al*., 1997; Wu *et al*., 1997). In the second model, Bcl-2s would also act by regulating the release of some caspase activators, as cytochrome c or Apoptosis Inducing Factor (AIF), usually sequestered in intracellular compartments (Susin *et al*., 1996; Kluck *et al*., 1997; Yang, *et al*., 1997). The observed pore-forming properties of some Bcl-2s suggest that these products would directly regulate the permeability of the intracellular mem-

Correspondence: J-L Vayssière
Received 18 August 1997; revised 1 April 1998; accepted 1 May 1998

branes (Muchmore *et al*., 1996; Minn *et al*., 1997; Schendel *et al*., 1997).

Given the complexity and diversity of caspase activation pathways, these experiments point to the mitochondrion as an unifying element of PCD (Golstein, 1997; Kroemer *et al*., 1997; Reed, 1997; Mignotte and Vayssière, 1998). Although for a long time the absence of mitochondrial changes was considered as a hallmark of apoptosis, mitochondria appear today as the central executioner of programmed cell death. Several reports suggest that mitochondria could be a crucial target in the apoptotic process, a point-of-no-return where different signal transduction pathways converge and beyond which a cell becomes irreversibly committed to death. Impairment in rnitochondrial function, an early event in the executive phase of PCD in different cell types, appears as the consequence of a preliminary reduction of the mitochondrial transmembrane potential ($\Delta\Psi$m) (Vayssière *et al*., 1994; Petit *et al*., 1995; Zamzami *et al*., 1995). The early $\Delta\Psi$m disruption would be the result of an opening of mitochondrial permeability transition pore (PTP) and this permeability transition would trigger the release of apoptogenic factors, as AIF or cytochrome c, capable of inducing the later apoptotic events (Kroemer *et al*., 1995; Zamzami *et al*., 1996).

This crucial position of mitochondria in PCD control is reinforced by results suggesting a more upstream involvement of mitochondria in PCD via the production of cell death signaling Reactive Oxygen Species (ROS). Indeed, several observations outline that these compounds may be central in the cell death transduction pathways of PCD triggered by a wide range of influences including UV light, ionizing irradiation, anthracyclines, ceramides, glucocorticoids or survival-factor withdrawal (Jacobson, 1996). In particular, the ability of endogenous or exogenous anti-oxidants to inhibit or delay PCD in some experimental systems appears as one of the compelling evidences of the contribution of ROS to the activation of the execution machinery (Wong, 1989; Sandstrom and Buttke, 1993; Mayer and Noble, 1994; Greenlund *et al*., 1995; Mehlen *et al*., 1996). The nature of the ROS involved in PCD is a conflicting question. Indeed, two opposite models have emerged in relation with the variety of metabolic reactions and intracellular sites which can generate ROS (Jacobson, 1996). While most investigators believe that oxidants are produced by electron chain transport, some data suggest that fatty acid metabolites, such as those produced from arachidonic acid by the lipoxygenase pathway, may be better mediators of PCD (O'Donnell *et al*., 1995). Nevertheless, these considerations do not refute the mounting evidence of the involvement of the mitochondrial electron transport chain in PCD-signaling ROS production. Thus, it was established that both ROS accumulation and PCD process require the presence of a functional mitochondrial respiratory chain in most ROS-dependent cell death systems (Schulze-Osthoff *et al*., 1993; Higuchi *et al*., 1997; Quillet-Mary *et al*., 1997).

To date, most of the progress in understanding PCD has been horizontal. However, major challenges remain in linking these expanding knowledges to integrate this pathway vertically. Of particular relevance would be insights into the connections between the molecular components involved in PCD and the physiological and morphological events associated with cell death. We have used the Tumor Necrosis Factor-α (TNF-α)-mediated cytotoxicity as a model for such an approach according to the data that outline the involvement of mitochondria, ROS and caspases in this cell death type.

One of the prominent features of this cytokine is its ability to kill several cell lines. Depending on the cell-type, TNF-α can induce both necrosis and PCD through complex signal transduction cascades initiated by the occupancy of the cell surface receptor TNFR1, and multiple intracellular pathways may be involved (Liu *et al*., 1996b). ROS appear as potent mediators of the killing activity of the cytokine (Goossens *et al*., 1995; Talley *et al*., 1995). The protective effect exerted by inhibitors or by elimination of the mitochondrial electron transport chain suggests that mitochondria could be the source of ROS production (Schulze-Osthoff *et al*., 1992, 1993). However, some other data provide evidence that the lipoxygenase pathway rather that the mitochondrial respiratory chain plays a central role in TNF-α-mediated cytolysis (O'Donnell *et al*., 1995). However, most of the data showing a requirement for ROS production in cell death activation would concern necrosis rather than PCD. It was assumed that TNF-α induces ROS formation and PCD by separate pathways, and that the ROS produced can lead to necrosis depending on other signals, intracellular redox status and levels of anti-oxidant protection (Jacobson, 1996). Thus, accumulation of high levels of ROS would induce necrosis, while PCD would be predominant in the presence of low levels of ROS.

A major advance in understanding early events in TNF-α signaling was the identification of proteins (TRADD, FADD and RIP) that are recruited to the cytoplasmic domain of TNFR1, following ligand induced trimerization (Nagata, 1997). Two death pathways have been identified: one mediated *via* FADD-induced recruitment of caspase-8, originally termed MACH/FLICE (Boldin *et al*., 1996) and the other linked to RIP and the possible recruitment, via its death domain, of another downstream effector molecule (Stanger *et al*., 1995; Boldin *et al*., 1996; Nagata, 1997). Caspase-8 could connect this complex and the cell death machinery, and so could be the most upstream enzymatic component in the TNF-α-induced cell death signaling cascades (Boldin *et al*., 1996). Other members of the caspase family, such as caspase-7 and caspase-3, could be substrates for caspase-8 cleavage. Involvement of multiple proteases in the cell death process is consistent with the reported ability of inhibitors of distinct caspases to protect cells from TNF-α-induced cell death (Beidler *et al*., 1995; Hsu *et al*., 1995; Miura *et al*., 1995; Duan *et al*., 1996).

The aims of the present study were (i) to examine the precise role and the source of ROS in the TNF-α-induced PCD, (ii) to characterize and order the morphological and mitochondrial changes associated with this process and (iii) to link these events with the activation of caspases. For this purpose, we monitored, by flow cytometry, the mitochondrial membrane potential and ROS formation in individual TNF-α-treated HeLa cells. Analyses were also performed on TNF-α-treated cells in the presence of an anti-oxidant,

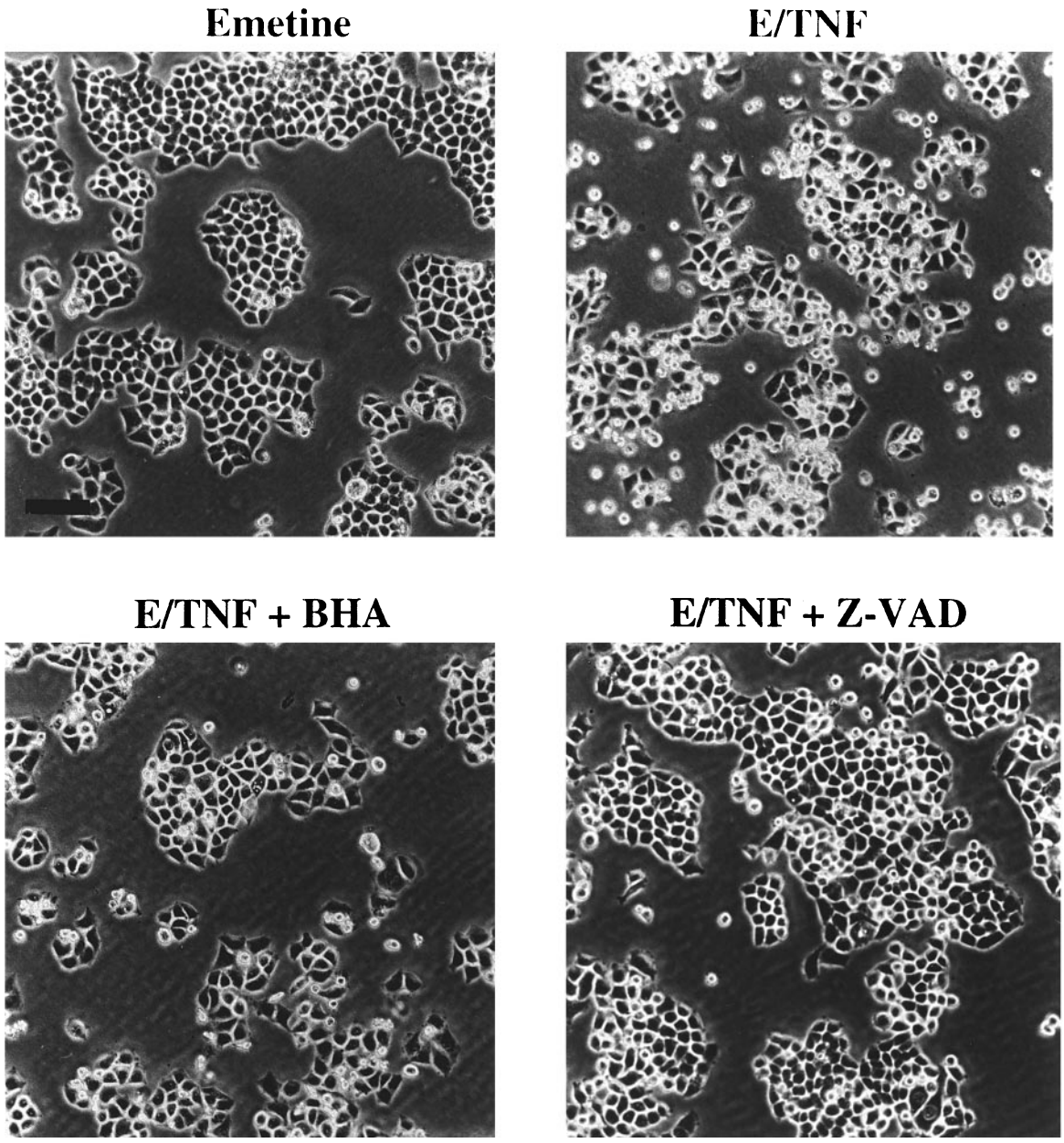

Figure 1 Morphological features of E/TNF induced HeLa cell death. Photographs of culture dishes were taken with a phase contrast microscope (scale bar equals 100 μm), after 6 h of emetine or E/TNF treatment. Pictures of cells treated with E/TNF in the presence of an anti-caspases (100 μM Z-VAD) or an anti-oxidant (100 μM BHA) are also included. The histogram reports the percentage of cell death obtained after 14 h of indicated treatment, assessed by trypan blue dye exclusion test

or of a general caspase inhibitor. To assess the role of mitochondria in the cell death signal transduction, these studies were also realized on HeLa-variant cell lines lacking functional mitochondrial respiratory chain. We show that at least two separate signaling cascades, one ROS-dependent and the other ROS-independent, contribute to the TNF-α-induced PCD of HeLa cells. ROS generation, an upstream event in the cell death process, requires functional mitochondria and is dependent on activation of caspase(s).

Results

TNF-α induces apoptosis in HeLa cells

TNF-α is a cytokine that causes *in vitro* cell death of several transformed cells. Depending on the cell type, TNF-α kills either by necrosis or apoptosis (Schulze-Osthoff *et al*., 1994). HeLa cells are resistant to cytolysis by TNF-α but can be sensitized by inhibition of protein synthesis. In order to characterize the pattern of HeLa cell death induced by TNF-α plus emetine as macromolecular synthesis inhibitor, we have analysed cytological alterations and DNA fragmentation upon treatment. The earliest changes observed were rounding up, phase-brightening and shrinkage of cells and blebbing of the plasma membrane (Figure 1). These events were observed after 4 h of treatment and preceded detachment, loss of refringence of the cells as well as fragmentation of DNA, as judged by flow cytometric analysis of TUNEL-stained cells (data not shown). These alterations massively occurred after 9 h of incubation with the drugs. Breaking up of the dead cells into fragments was the latest event observed, but it affected only few dead cells. All these morphological and molecular changes are characteristic features of apoptosis (Kerr *et al*., 1972). This morphological study as well as the following experiments were also performed in the presence of a synthetic caspases inhibitor or in the presence of an anti-oxidant. To avoid redundancy, the effects of these compounds will be presented in specific paragraphs.

A two-step process in ROS generation is associated with TNF-α-induced apoptosis

In order to assess ROS production in individual cells during apoptotic cell death induced by TNF-α, flow cytometric analysis was carried out using DCFH-DA as fluorescent probe (see Material and methods). In parallel, with the aim to compare the kinetic of changes in ROS production to the evolution of a well established early hallmark of apoptosis, a similar study was performed concerning the $\Delta\Psi$m, using $DiOC_6(3)$ as fluorochrome (Vayssière *et al*., 1994; Petit *et al*., 1995; Zamzami *et al*., 1995). In all measures, cell plasma membrane integrity was also assessed by staining cells with PI (see Materials and methods).

Figure 2 depicts typical cytograms (where each cell analysed is represented by a dot) obtained with multiparametric flow cytometric analysis of control or emetine/TNF-α (E/TNF)-treated cells. For each sample analysed, light scatter properties of cells, i.e. cell size (FSC) *versus* cell density (SSC), are recorded and allow exclusion of cell debris or aggregates from the $DiOC_6(3)$ or DCF fluorescences analysis.

A two-step process was observed concerning the evolution of $DiOC_6(3)$ and DCF fluorescences during E/TNF treatment (see Figure 2, cytograms FSC *versus* $DiOC_6(3)$ or DCF). Indeed, for each staining, two new cell clusters successively appeared after E/TNF addition. For $DiOC_6(3)$ fluorescence, a fraction of cells underwent a first reduction in tracer retention as compared to control cells, immediately followed by a second decrease. These populations have been classified as follows: (i) DiOC-medium cells are cells with intermediate loading (four times less than control cells) and (ii) DiOC-low, cells are cells presenting the lowest staining (thirty times less than control cells). Conversely, for DCF fluorescence, a fraction of cells presented a first increase in DCF production (three times more than untreated cells) followed by a second higher increase in DCFH-DA oxidization (ten times more than untreated cells). These populations are respectively named DCF-medium and DCF-high cells.

Figure 3 shows the evolution of the percentages of these distinct cell populations during the E/TNF treatment. From data plotted on the upper panel, it appears that globally, the percentages of $DiOC_6(3)$-negative cells (sum of DiOC-medium and -low cells) and DCF-positive cells (sum of DCF-medium and -high cells) evolve identically during E/TNF treatment. Analysis of the stack histograms (Figure 3, middle and lower panels) detailing the respective part of $DiOC_6(3)$-medium and -low cells (or DCF-medium and -high cells) to the global percentage of $DiOC_6(3)$-negative (or DCF-positive) cells appearing during treatment has led to the following conclusions: (i) the appearance of DCF-medium cells corresponding to the first increase in ROS production was correlated with the appearance of DiOC-medium cells that result from the first drop of $\Delta\Psi$m; (ii) the second fall of $\Delta\Psi$m arose immediately after the first one in such a way that it appeared as the consequence of a magnification process; (iii) the second burst in ROS production giving DCF-high cells was clearly time distinct from the first increase and followed the second loss of $\Delta\Psi$m leading to DiOC-low cells; (iv) the TNF-α-induced responses evolve asynchronously in the cell population.

These flow cytometric data were performed on whole cell population, i.e. adherent but also floating cells (not visible before 9 h of treatment). At this time, separate analysis of adherent and floating cells showed that while all floating cells demonstrated higher DCF fluorescence and lower $DiOC_6(3)$ fluorescence, only some adherent cells presented these features (data not shown). Thus, the appearance of DiOC-low and DCF-high fluorescences preceded detachment and loss of the refringence of the E/TNF treated cells that characterize the destruction phase of the process.

In view of these results, we investigated the relationship between these changes and morphological events associated with the cell death process. At different time points, E/TNF-treated cells were double-loaded with either $DiOC_6(3)$/DAPI or DCFH-DA/DAPI and examined by epifluorescence. After 4 h of E/TNF treatment, as indicated by arrows in Figure 4, cells with enhanced DCF fluorescence and cells with lower and differently distributed $DiOC_6(3)$ fluorescence could be detected, their number increasing as a

function of time. Moreover, these changes correlated with rounding up of the cell and nuclear condensation monitored with the DAPI fluorescence. Although all cells with these morphological apoptotic features showed fluorescence changes and all cells with lower $DiOC_6(3)$ fluorescence harbored morphological modifications, there were some cells exhibiting an increase in DCF fluorescence with intermediate alterations, i.e. with progressing morphological alteration but without nuclear condensation (Figure 4, arrowheads). These observations show that the drops of the $\Delta\Psi m$ are associated with the progress of morphological features that characterize apoptosis while the first increase in ROS generation could constitute a primary event preceding the commitment to the cell death process.

ROS constitute mediators of one of the two TNF-α-activated signaling cascades

To further document the role of ROS in TNF-α-induced cytotoxicity, the scavenging of TNF-α-induced ROS by BHA, a potent anti-oxidant, was analysed together with its capacity to protect cells against TNF-α-induced apoptosis. When BHA was added at the same time as TNF-α, ROS accumulation was greatly delayed and reduced (Figure 5b) as was cell killing (Figure 1, photograph and histogram). Moreover, the commitment to the cell death process observed in the presence of this anti-oxidant was ROS-independent: the loss of the $\Delta\Psi m$ and the morphological changes occurred before an increase in ROS generation (Figure 5a compared to 5b). However, under these conditions, the terminal phase of cell destruction was always associated with an accumulation of ROS that could not be scavenged by BHA. This observation suggests that ROS produced during the activation and the destruction phases are of different types. Taken together, these results support the idea that two separate signaling cascades are activated by TNF-α in HeLa cells, one ROS-dependent and the other ROS-independent. Moreover, the comparison of the kinetic and of the extent of cell death process in the presence

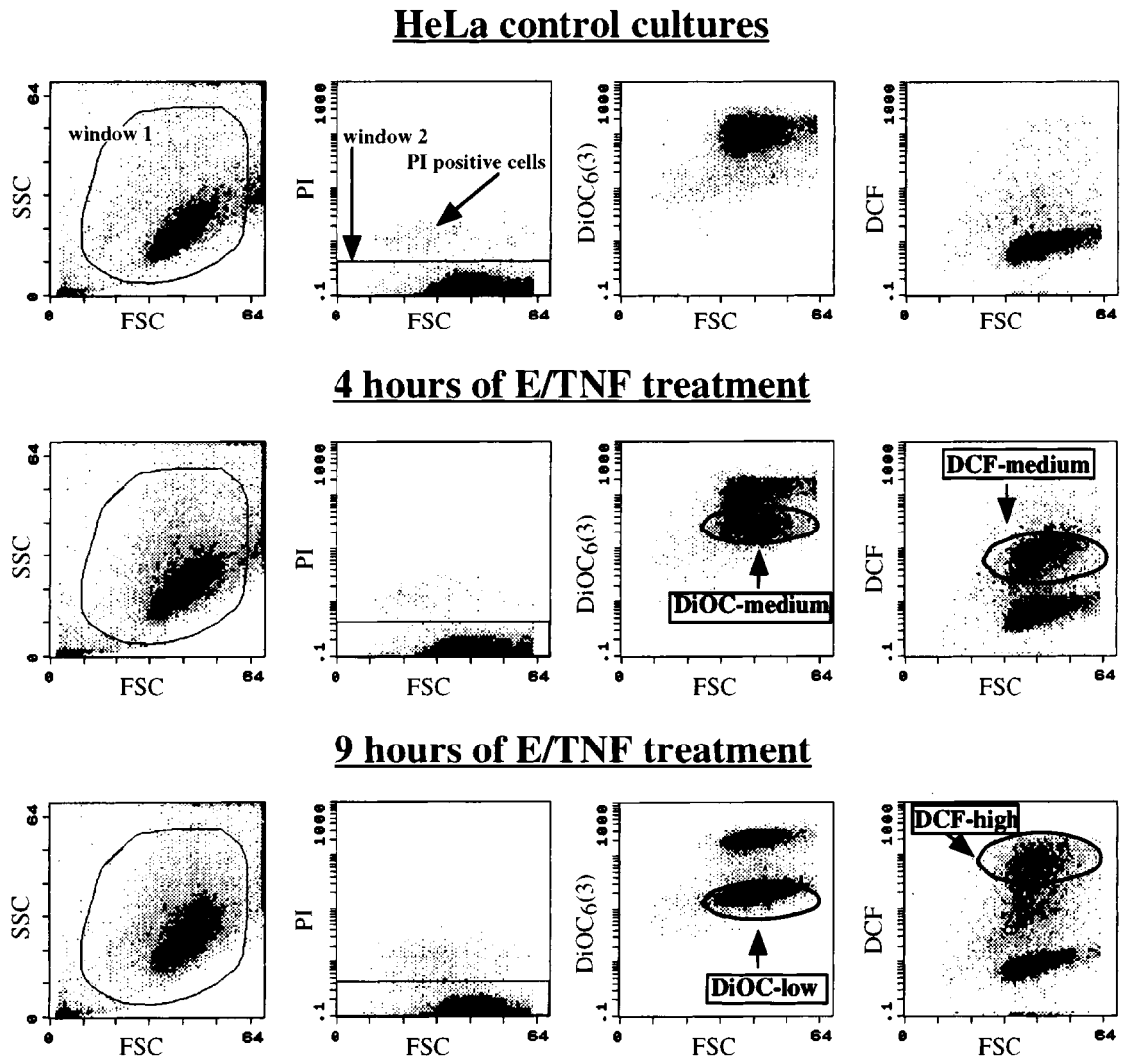

Figure 2 Multiparametric analysis of HeLa cells by flow cytometry. The data shown, where each cell is represented by a dot, are relative to control cells (upper panel) and cells treated for 4 h (middle panel) or for 9 h (lower panel) with E/TNF. For each sample analysed, light scatter properties of the cells were recorded (cytogram FSC *versus* SSC) together with the PI fluorescence, represented in the cylogram FSC *versus* PI. The mitochondrial membrane potential, measured by the $DiOC_6(3)$ fluorescence, and the ROS production, measured by the DCF fluorescence, are reported. These latter cytograms are gated on the cell population of interest (window 1) and on PI negative cells (window 2)

and in the absence of anti-oxidant suggests that the ROS-dependent pathway is nevertheless predominant and proceeds more rapidly that the other one (Figure 1 and 5a).

With the aim to assess the effect of ROS accumulation on cellular redox potential, we have measured the fate of the redox modulator glutathione (GSH) in E/TNF-treated HeLa cells. For this purpose, flow cytometric analysis were carried out using monobromobimane (mBBr) as specific probe. Cellular appearance of GS-mBBr fluorescence was monitored and results obtained are depicted in Figure 6. The intracellular GSH content of HeLa cells was observed to fall after exposure to E/TNF (Figure 6a), the mean fluorescence of mBBr-negative cells being three times less than that of control cells. The evolution of the percentage of mBBr-negative cell population (plotted in Figure 6b) is correlated with the appearance of DCF-positive cells during E/TNF treatment (see Figure 5b). When BHA was added at the same time as E/TNF, GSH depletion was greatly delayed and reduced, suggesting that ROS produced are responsible for GSH depletion.

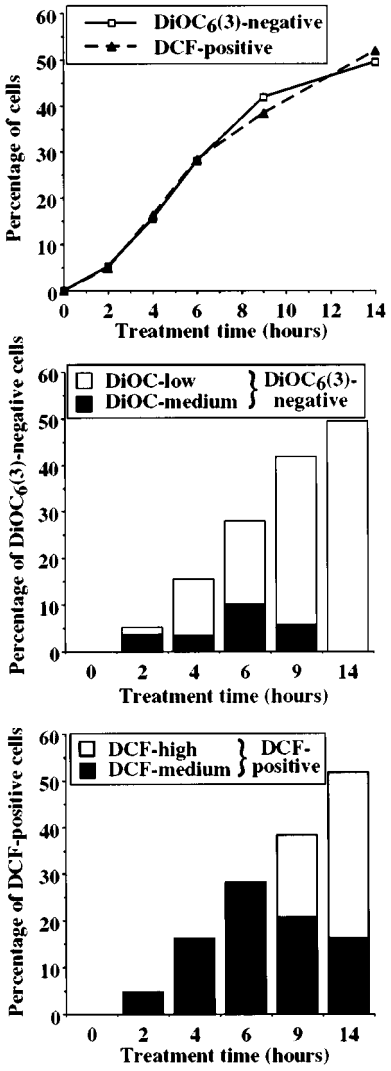

Figure 3 Evolution of the membrane potential and ROS production during E/TNF-induced apoptosis of HeLa cells. The upper panel is relative to the percentage of $DiOC_6(3)$-negative (composed of DiOC-medium and DiOC-low cells) and DCF-positive (comprising DCF-medium and DCF-high cells) HeLa cells, recorded at indicated times after induction of apoptosis. The middle panel shows a stack histogram allowing to distinguish, among the $DiOC_6(3)$-negative cells, the percentages of DiOC-medium and DiOC-low cells that appear during treatment. The lower panel is a stack histogram detailing the respective part of DCF-medium and DCF-high cells to the global percentage of DCF-positive cells appearing during treatment. All these data are derived from cytometric analysis (see Figure 2)

Rho⁰ HeLa cells are less sensitive to TNF-α-induced cytotoxicity

In order to investigate the involvement of mitochondria in the initial generation of ROS during TNF-α-induced cell death, we have isolated subclones of HeLa cells that are deficient in a functional respiratory chain. Respiration deficiency was generated by long-term culture of HeLa cells in ethidium bromide (EtB) containing medium, a procedure which has been repeatedly used to deplete cells of mitochondrial electron systems (Desjardins *et al*., 1985; King and Attardi, 1989), as EtB has been described as a specific inhibitor of mitochondrial DNA (mtDNA) replication. Several subclones of EtB-resistant cells were isolated and controlled for mtDNA depletion (data not shown). Two rho⁰ clones, namely B4 and B5, were retained for this study. Only results obtained with rho⁰ B4 cell line are presented as both rho⁰ clones gave similar responses.

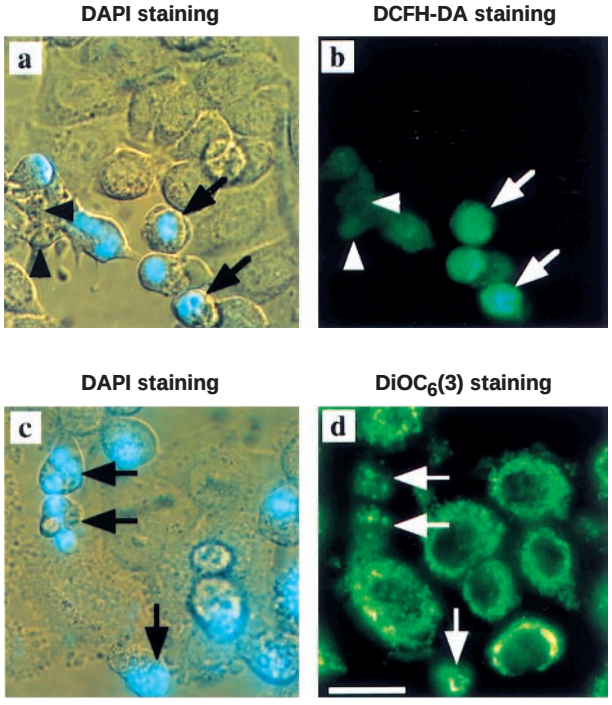

Figure 4 Visualization of the mitochondrial network and ROS production in E/TNF HeLa treated cells. After 4 h of E/TNF treatment, the mitochondrial network is visualized by staining cells with $DiOC_6(3)$ (**d**), whereas the ROS producing cells are assessed after staining with DCFH-DA (**b**), as described in Material and methods. In parallel, nuclear condensation was monitored with the DAPI fluorescence (**a**, **c**). Photographs (scale bar equals 20 μm) were taken with a fluorescent microscope (DMRB Leica) and are representative of three distinct experiments, in each of which approximately ten pictures were examined

Transmission microscopy showed that E/TNF killed rho^0 HeLa cells and that this death harbored the same morphological features as the E/TNF-induced cell death of rho$^+$ HeLa cells, i.e. apoptosis. However, we observed that fewer rho^0 cells died as compared to rho$^+$ HeLa cells. Similar conclusions could be drawn from the flow cytometric study which showed that a smaller fraction of rho^0 cells presented the characteristic changes of the TNF-α-induced cytotoxicity as compared to rho$^+$ HeLa cells (Figure 7a). Moreover, it should be noted that in rho^0 cells, ROS-accumulation took place after the loss of ΔΨm and the onset of the cell death process, and was not scavenged by BHA (Figure 7c). This ROS accumulation is in fact associated with the onset of the destruction phase and must correspond to the second burst described in rho$^+$ cells. Furthermore, addition of BHA has little or no effect on the kinetic and the extent of cell death (Figure 7b). Therefore, activation of the TNF-α-induced apoptotic program in rho^0 cells does not require ROS production. In conclusion, as the ROS-dependent pathway is not effective in rho^0 cells, it can be assumed that the production of ROS involved in the activation phase of this signaling cascade is dependent on the presence of a functional respiratory chain, indeed even that ROS are produced by mitochondria.

The two TNF-α-induced signaling cascades require an upstream activation of Z-VAD sensitive caspase(s)

Several caspases have been assumed to mediate TNF-α cytotoxicity (Nagata, 1997). Caspase-8 appears as an upstream component of the cell death signaling cascade leading to the activation of caspases-3 or -7 which would be part of the killing machinery (Beidler *et al*., 1995; Miura *et al*., 1995). In order to compare the

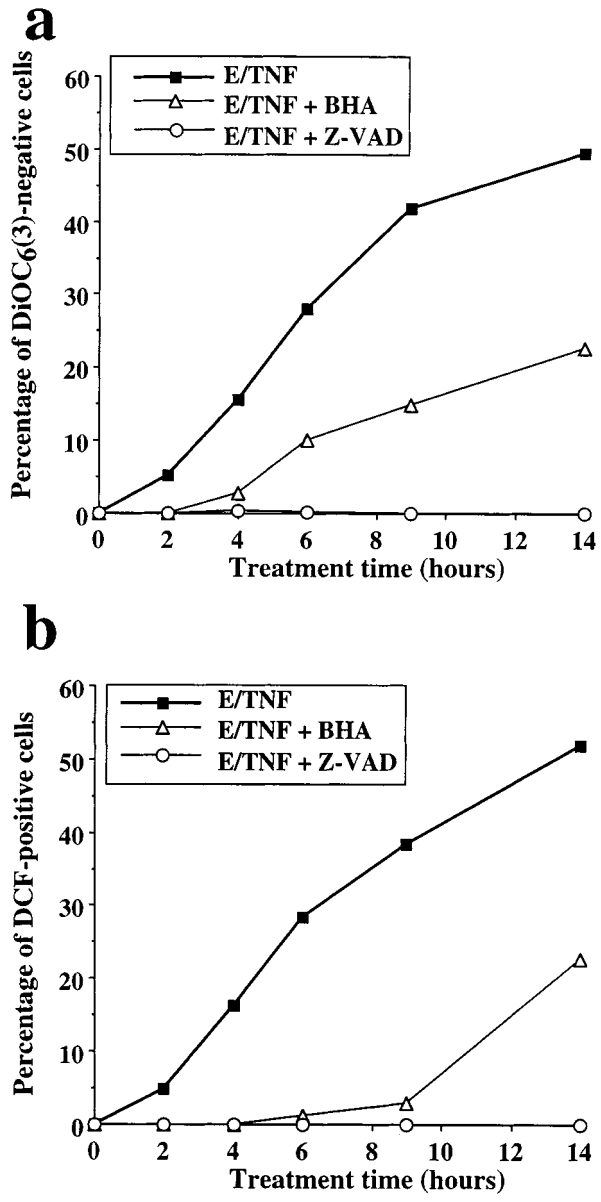

Figure 5 Protective effect of an anti-oxidant and of an anti-caspases on the drop of ΔΨm and the ROS production during E/TNF treatment. (**a**) depicts the percentage of $DiOC_6(3)$-negative cells calculated at indicated times after cells were treated with E/TNF alone or in the presence of an anti-oxidant (100 μM BHA) or an anti-caspases (100 μM Z-VAD). (**b**) is relative to the percentage of ROS producing cells recorded at indicated times after cells were treated with E/TNF with or without BHA or Z-VAD. Data are derived from flow cytometric analysis

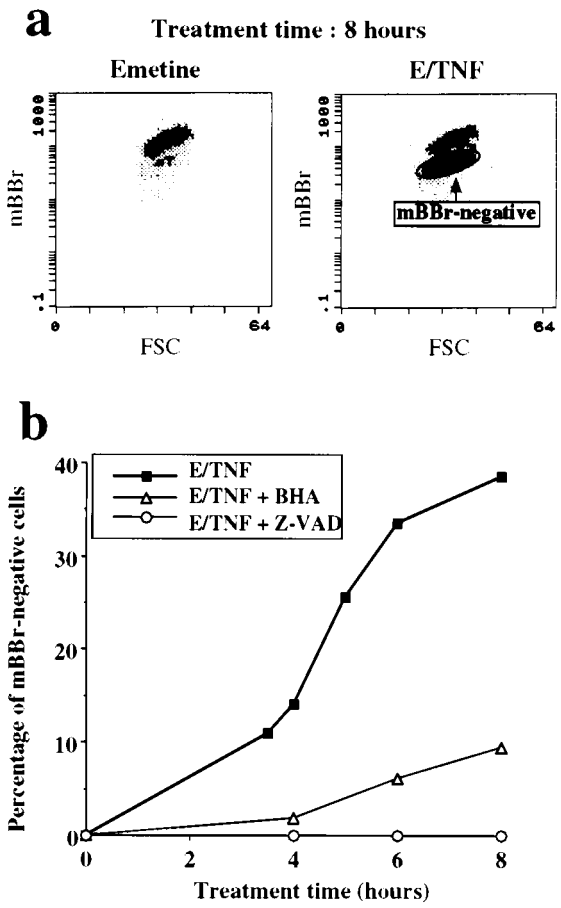

Figure 6 Fate of GSH during E/TNF-induced apoptosis. (**a**) depicts typical cytograms (FSC *versus* GS-mBBr fluorescence) obtained with flow cytometric analysis of emetine or E/TNF treated HeLa cells. Data plotted in panel b are derived from cytometric analysis and show the evolution of the percentages of mBBr-negative cell population upon E/TNF treatment. Results obtained when the anti-oxidant BHA of the anti-caspases Z-VAD are added at the same time as E/TNF are included

relative involvement of caspases in the two described TNF-α-activated transduction pathways in HeLa cells, we have investigated the relationship between caspases and the physiological and biochemical events of the TNF-α-induced apoptosis. For this purpose, we have analysed the effect of Z-VAD, a general caspase inhibitor on the morphological changes, the ROS production and the mitochondrial membrane potential loss observed during the E/TNF treatment of HeLa cells.

When Z-VAD was added to rho$^+$ HeLa cells at the same time as E/TNF, ΔΨm loss and ROS accumulation were totally blocked (Figure 5a and b) as was cell shrinkage and cell killing (Figure 1, photograph and histogram). This result is in agreement with the substantial evidence implicating caspase-8, a Z-VAD sensitive caspase (Martin *et al*., 1998), in a primary

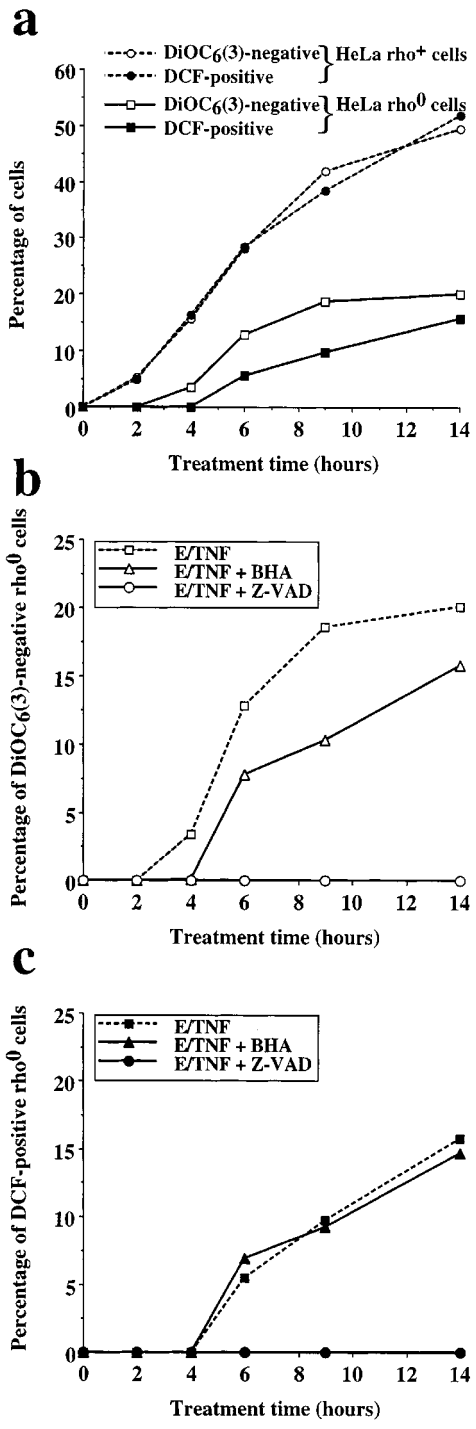

Figure 7 Flow cytometric analysis of ROS production and ΔΨm of HeLa rho^0 cells treated with E/TNF. (**a**) Percentage of $DiOC_6(3)$-negative and DCF-positive cells recorded at indicated times after E/TNF treatment. Results obtained with HeLa rho$^+$ cells and HeLa rho^0 cell line (clone B4) are represented. (**b**) Percentage of $DiOC_6(3)$-negative cells in HeLa rho^0 cultures treated with E/TNF alone or in the presence of the anti-protease Z-VAD (100 μM) or the anti-oxidant BHA (100 μM). (**c**) Data plotted are relative to the percentage of DCF-positive HeLa rho^0 cells appearing upon treatment with E/TNF with or without Z-VAD or BHA. These data are obtained from flow cytometric analysis

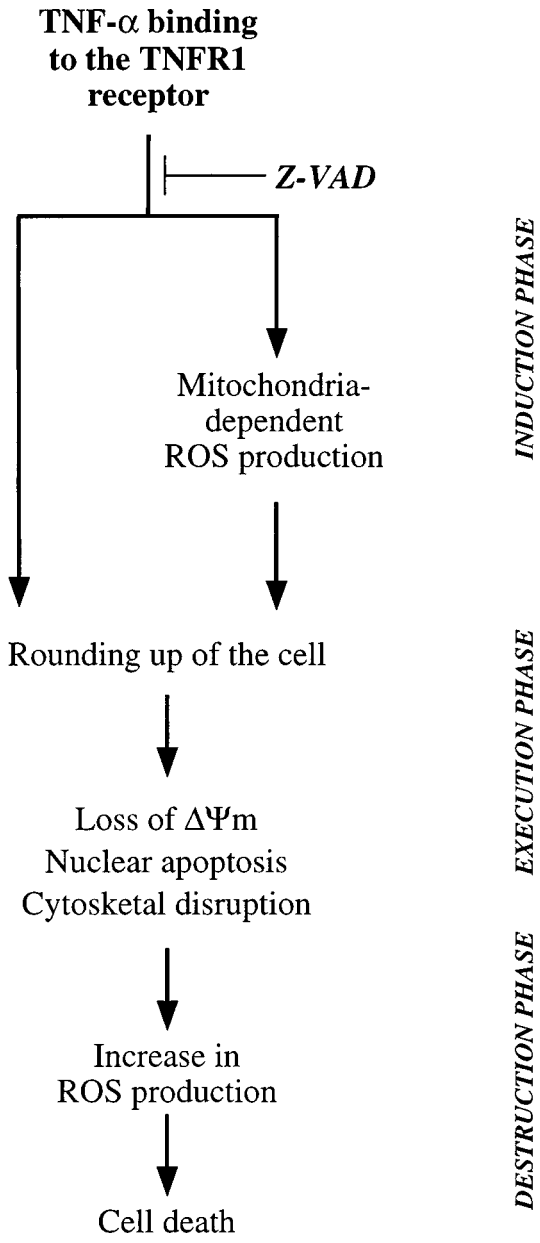

Figure 8 Relative order of biochemical and physiological events associated with the two TNF-α-induced cell death pathways. This schematic model takes into account the different observations obtained from the studies of the effects of a synthetic caspases inhibitor and of an anti-oxidant on distinct hallmarks of the TNF-α-induced cell death (see Results)

phase of the TNF-α-induced apoptosis (Miura *et al*., 1995). Here, we show that activation of caspase(s) takes place upstream from the appearance of DCF-medium cells, i.e. in the activation phase of the ROS-dependent pathway. That caspases are also involved in the activation phase of the ROS-independent signaling cascade was supported by the following observations: (i) $DiOC_6(3)$-negative cells do not appear in the presence of Z-VAD while they appear after 4 h in the presence of BHA (Figure 5a), where the ROS-independant pathway predominates; (ii) the protective effect against cell death is higher with Z-VAD than with BHA (Figure 1, photograph and histogram); (iii) Z-VAD inhibits cell death observed in the presence of BHA (data not shown) and (iv) Z-VAD could efficiently protect rho^0 HeLa cells from loss of $\Delta\Psi m$ and ROS production (Figure 7b and c) and from cell death (data not shown).

Discussion

TNF-α activates multiple apoptosis signaling pathways, one of which is mediated by ROS

In our study, we have investigated the role of ROS in TNF-α-induced PCD of HeLa cells. Indeed, TNF-α-treatment of HeLa cells provoked the appearance of the characteristic morphological and molecular features of apoptosis. The kinetic study of the process allowed us to precisely define three distinct phases: (i) the activation phase, during which no macroscopic changes could be observed; (ii) the execution phase, where the morphological apoptotic changes arise (rounding up and shrinkage of the cell, condensation and subsequent fragmentation of the chromatin, disruption of the cytoskeleton and blebbing of the plasma membrane) and lastly; (iii) the destruction phase characterized by the detachment, the loss of refringence of the cell and by the terminal fragmentation of nuclear DNA. In order to clarify the role of ROS in this apoptotic model, we have analysed with flow cytometry the production of intracellular ROS. This method revealed two 'time-distinct' increases in ROS accumulation: the first increase, that could be responsible for GSH depletion in our model, could be associated with the commitment of cells into the apoptotic process while the second one preceded the terminal phase of destruction of the cells. Moreover, epifluorescence microscopy examination showed that the first observed ROS accumulation could be more precisely correlated with the activation phase of the cell death program. Hence, with the aim to clarify the contribution of ROS in this early phase, we tested the effect of the synthetic ROS scavenger BHA on the TNF-α-induced apoptosis. BHA delays and reduces the first observed ROS accumulation and protects against TNF-α cytotoxicity. However, some cells nevertheless died in the presence of the anti-oxidant. These cells did not harbor this first ROS production preceding the commitment to cell death but exhibited the morphological features of apoptosis. These results allow us to suggest that two separate transduction pathways are activated by TNF-α in HeLa cells, one involving ROS and the other ROS-independent. Moreover, it appears that the ROS-mediated signaling cascade is predominant and that it proceeds more rapidly than the ROS-independent pathway. To our knowledge, although ROS are clearly involved in TNF-α-induced necrosis this is the first time that clear evidence of such a crucial role for ROS is established in TNF-α-induced apoptosis. These data could be related to the existence of a negative feedback mechanism associated with TNF-α-signaling in which NF-κB activation suppresses the signal for cell death (Beg and Baltimore, 1996; Liu *et al*., 1996b; Van Antwerp *et al*., 1996; Wang *et al*., 1996). This protective effect was assumed to be linked to the induction of anti-apoptotic genes by NF-κB. Among the NF-κB-transcriptonally up-regulated genes, is the gene encoding the manganese superoxide dismutase, an enzyme that takes part in the anti-oxidant defense system developed by all aerobic cells. In relation with our data, it can be assumed that, in the presence of macromolecular synthesis inhibitors, the sensitivity of HeLa cells to TNF-α-induced cell killing would result from their inability to scavenge the increased ROS production triggered by the TNFR1 activation.

Our study also revealed the existence of a second step of ROS accumulation which appeared as a late event of the execution phase of the apoptotic process, just preceding the terminal destruction of the cell. This ROS production was observed in the rho^+ HeLa cells as well as in the rho^0 ones, suggesting that it occurs independently from the mitochondrial respiratory chain. This result can be linked to the following observations: (i) these compounds, unlike the activation phase–associated ROS, are not scavenged by the synthetic BHA and; (ii) they can oxidize hydroethidine while the former do not (data not shown). Therefore, we can assume that the ROS produced during these two steps are of different types. The significance of this secondary ROS increase in the TNF-α-induced apoptosis is unclear; indeed, it may correspond to a side effect of the process or, conversely, to a crucial event involved in the destruction of the cellular structures.

Functional mitochondria are required for the ROS-dependent signaling pathway

Another problem that we have approached in our study concerns the conflicting question of the source of ROS mediating the TNF-α-induced cell death. Most investigators believe that oxidants are generated by the mitochondria as a result of an early alteration of the mitochondrial respiratory chain (Schulze-Osthoff *et al*., 1993). The protective effect exerted by inhibitors or by elimination of electron transport chain provide major arguments for this model. However, it was also suggested that fatty acid metabolites, such as those produced from arachidonic acid by the lipoxygenase pathway, rather than mitochondrial ROS, are messengers of the TNF-α-induced cytotoxicity (O'Donnell *et al*., 1995).

We have assessed the role of mitochondria in the ROS-dependent signaling cascade, by examining the requirement of the mitochondial respiratory chain (the source of mitochondrial ROS production) in the TNF-α-induced cell death pathway. For this purpose, we isolated mitochondrial DNA-depleted subclones of HeLa cells. The obtained rho^0 cells presented a

marked resistance towards TNF-α cytotoxicity which corresponded to an inhibition of the ROS-dependent signaling pathway while the ROS-independent one was always effective. While these cells showed a slightly different morphology and a reduced growth rate, they did not however reveal any significant modification of TNF-α receptor numbers as measured by Western blot using specific antibodies (data not shown). The existence of one mitochondrial respiratory chain-independent pathway would explain why some rho^0 cells are sensitive to TNF-α (Gamen *et al*., 1995; Marchetti *et al*., 1996) while others are not (Higuchi *et al*., 1997). The ability of a rho^0 cell to undergo apoptosis would necessitate a functional ROS-independent pathway which could be cell type specific.

The resistance of rho^0 cells did not correlate with a more effective anti-oxidant defense system as ascertained by their higher sensitivity to externally applied hydrogen peroxide than their counterpart rho^+ cells (data not shown). Thus the acquired resistance of rho^0 cells to TNF-α treatment outlines the crucial role of mitochondria in the major TNF-α-induced killing pathway as the probable source of ROS involved in the activation phase of this process. However these results do not demonstrate that mitochondrial ROS are messengers of the death signaling cascade. An alternative explanation would consider that mitochondrial ROS or other mitochondria-derived intermediates could be required in the pathway that leads to the accumulation of ROS produced elsewhere. Thus, the mitochondrial ROS, which are usually generated in active mitochondria, could activate some metabolites that accumulate in response to the TNF-α treatment. The generation of the highly, reactive peroxinitrite provides a good example for this hypothesis, in the way that it results from the reaction between the mitochondria-produced superoxide anion and the cytoplasmic nitric oxide (Packer and Murphy, 1994).

What is the mechanism leading to the accumulation of mitochondrial ROS? Much of the available data converge to the hypothesis that ROS increases are the consequence of an impairment of the mitochondrial respiratory chain (Schulze-Osthoff *et al*., 1992; Gudz *et al*., 1997; Quillet-Mary *et al*., 1997; France-Lanord *et al*., 1997). Indeed, it was shown that an upstream inhibition, with chemical compounds acting on complex I (Schulze-Osthoff *et al*., 1992; Quillet-Mary *et al*., 1997), or an elimination of the electron transfer chain (Schulze-Osthoff *et al*., 1993; Higuchi *et al*., 1997), by depletion of the mtDNA, prevent ROS accumulation and consequently protect cells against PCD. The ubiquinone site in complex III appears as the major site of mitochondrial ROS production as this site catalyzes the conversion of molecular oxygen to superoxide anion which can lead to the formation of other potent ROS such as hydrogen peroxide and hydrogen radicals. Such a model is supported by the observed potentiation of cell death processes in ROS-dependent PCD when electron flow was inhibited distal to the ubiquinone pool. In agreement with the above considerations, the observed alterations are distal to the ubiquinone site of the complex III, but the origin of these electron flow disturbances are not clear. The only strong evidence comes from the study of ceramide-induced PCD, in which an increased H_2O_2 production was linked to mitochondrial Ca^{2+} homeostasis perturbation as inhibition of the mitochondrial Ca^{2+} uptake was shown to abolish both ROS accumulation and cell death (Gudz *et al*., 1997; Quillet-Mary *et al*., 1997; France-Lanord *et al*., 1997). However, the recently observed shift of cytochrome c from mitochondria to cytosol in the early phases of many PCD (see below) could provide a clue to resolve this question (Liu *et al*., 1996a; Kluck *et al*., 1997; Yang *et al*., 1997). Indeed, the release of cytochrome c must lead to a breakdown of the mitochondrial electron flow downstream of the ubiquinone site which in turn would result in an increased generation of ROS. Such a model is supported by the described correlation between loss of cytochrome c in respiratory failure in a Fas-induced PCD model (Krippner *et al*., 1996).

Caspases are the core components of the two TNF-α-induced signaling cascades

We have shown that Z-VAD-sensitive caspase(s) are involved in the early stages of the apoptotic program leading to the activation of the execution machinery. Moreover, these caspases constitute part of the two, ROS-dependent and ROS-independent, cell death signaling pathways that we have shown to be activated by TNF-α in the rho^+ HeLa cells. According to the protein recruitment model for TNF-α killing, this activity would correspond to caspase-8 whose recruitment to the cytoplasmic domain of TNFR1 allows its autoactivation and initiates a protease cascade leading to dismantlement of the cell (Nagata, 1997). This hypothesis is reinforced by the elsewhere described sensitivity of caspase-8 to Z-VAD (Martin *et al*., 1998). How can the existence of two pathways similarly sensitive to the Z-VAD inhibitor be integrated in this model? One possibility is that the two TNF-α-induced transduction cascades diverge downstream of caspase-8 and correspond to the activation by proteolytic cleavage of components able to activate by different routes the executors of the apoptotic program. Protein kinases, sphingomyelinases or phospholipases that have been shown to be activated in response to TNF-α could be potential targets for caspase-8 and mediators of the death signal. A second possibility is that TNF-α triggers two apoptotic pathways that diverge from the cytoplasmic domain of TNFR1, in relation with the FADD- and RIP-mediated recruitment of distinct death effector molecules. These two routes, one leading to ROS production and the other one not, would involve distinct caspases, namely caspase-8 and caspase-2. However, the observations that dominant negative FADD (Chinnaiyan *et al*., 1995) or MACH (Boldin *et al*., 1996) can completely inhibit apoptosis make this second model uncertain. Recently, such a 'two signaling pathways' model has been described in CD95-mediated PCD (Scaffidi *et al*., 1998), suggesting that this phenomenon could be a general feature of apoptosis induced *via* the transmembrane receptors of the TNF family (Nagata, 1997).

Furthermore, the finding that ROS play a crucial role in the transduction of the death signal downstream of the TNFR1-recruited caspase(s) during the initial phase impede the model of pro-apoptotic protease

cascade where caspases are presumed to exist within hierarchies of auto- and trans-cleavage (Fraser and Evan, 1996). Our results suggest the existence of at least one more indirect, ROS-dependent, mechanism for the activation of the execution caspases which constitute the core of the killing machinery. This observation is consistent with the observed caspase-independent activation of execution machinery (caspase-3) in many diversely triggered PCD (McCarthy, *et al*., 1997), and allow us to propose that the proteases cascade would not be the predominant way to activate the executor caspases.

Role of ROS in cell death signaling

The involvement of mitochondrial ROS in cell death transduction pathway leads to the fundamental questions concerning the molecular mechanisms underlying the ROS signaling, in particular how ROS mediate activation caspases of the cell death machinery. Two models can be proposed to approach this conflicting and not well documented subject. The first model assumes that ROS themselves are signaling molecules which activate some crucial components of the PCD machinery. Conversely, the alternative proposition suggests that ROS can act indirectly by modifying the cellular redox potential, which would regulate some key regulatory proteins involved in PCD. Note that the observations that we have made in TNF-α-induced killing of HeLa cells suggest that ROS produced provoke an oxidative stress via GSH depletion. Several lines of evidence confirmed by much of the available data agree with an explanation based on indirectly mediated action. First, unlike fatty acid metabolites which harbor specific reactivity and are known to mediate particular signals from surface receptors, mitochondrial ROS are characterized by a lack of biological specificity or even an extreme reactivity, as for the hydroxyl radical: these are all features contrary to the requirement of a specific signaling role (Jacobson, 1996). In this way, a direct influence of ROS on PCD process would be correlated to a general damaging effect on cellular structures resulting in necrotic cell death, or perhaps to a more limited action on mitochondria, their site of production, which in turn could activate some mitochondria-dependent downstream cascades leading to PCD. Secondly, despite the compelling evidence on the role of mitochondrial ROS in PCD signaling pathways, the prevalent idea is nevertheless that they do not represent a general mediator of cell death, as suggested by the ability of some PCD to occur in very low oxygen environments (Jacobson and Raff, 1995; Shimizu *et al*., 1995). However, an alternative approach to this problem would be to consider that the major effect of an increased ROS production is the subsequent decreased availibility of intracellular anti-oxidants as NADH, NADPH or glutathione, leading to imbalance of redox status which would be the central common effector of PCD. Anti-Fas/APO-1 antibody or interleukin-3 (IL-3) withdrawal-induced PCD represent good illustrations of this model (van den Dobbelsteen *et al*., 1996; Bojes *et al*., 1997). Indeed, no ROS accumulation can be measured in these two systems and anareobic cultured cells deprived of IL-3 still undergo PCD (Schulze-Osthoff *et al*., 1994; Shimizu *et al*., 1995). However, an oxidative stress can be shown in these models with a depletion of glutathione resulting from its rapid and specific efflux. This event takes place at the very beginning of the apoptoptic process (van den Dobbelsteen *et al*., 1996; Bojes *et al*., 1997). Moreover, it has been shown that Bcl-2 can protect cells from PCD by shifting the cellular redox potential to a more reduced state (Ellerby *et al*., 1996). However, the observation that oxidation of thiols other than glutathione can mediate induction of PCD suggest that the intracellular thiol redox status would be the real key factor of the cell death signaling pathways (Kane *et al*., 1993; Sato *et al*., 1995; Marchetti *et al*., 1997; Mirkovic *et al*., 1997). In this model, the redox state of glutathione or other cellular anti-oxidants such as thioredoxine, would be in equilibrium with that of thiols resident in some redox sensitive crucial components of the execution machinery as execution caspases (Kroemer *et al*., 1997; Mignotte and Vayssière, 1998). Where does ROS fit this thiol hypothesis? In this putative model, an increased production of mitochondrial ROS would result, either by a direct modification of the thiols or indirectly *via* a depletion of the intracellular anti-oxidant pool, in a shift of the redox state of the sensor SH groups to a more oxidized state. The nature of the ROS and the level of the intracellular anti-oxidant defenses would determine in which way regulatory components are activated to commit cells to PCD.

Conclusions

In conclusion, we have shown that binding of TNF-α to TNFR1 triggers multiple death signaling cascades, one of which being mediated by ROS, that nevertheless converge to a common apoptotic cell death (Figure 8). Each one of these pathways involves an early activation of Z-VAD-sensitive caspase(s), which regulate downstream the engagement of the execution process. Finally, our results also help to define the exact importance of mitochondria in the TNF-α-induced cell death process. Indeed, we show on the one hand that mitochondria play a key role in the ROS-dependent signaling pathway and, on the other hand, that mitochondrial membrane depolarization constitutes a caspase-dependent event of the execution stage which could then determine the downstream progress of the cell death program.

Materials and methods

Reagents

3,3′-diethyloxacarbocyanine ($DiOC_6(3)$), monobromobimane (mBBr) and dichlorofluorescin diacetate (DCFH-DA) were purchased from Molecular Probes (Eugene, OR, USA). Butylated hydroxyanisole (BHA), propidium iodide (PI), diamidino phenylindole (DAPI), recombinant TNF-α (2×10^7 units/mg) were from Sigma (St Louis, Mo, USA). Stock solutions of BHA, DCFH-DA, mBBr and $DiOC_6(3)$ were prepared in ethanol. DAPI, PI and TNF-α were dissolved in water. Z-Val-Ala-DL-Asp-Fluoromethylketone (Z-VAD) was from Bachem (Bubendorf, Switzerland) and was prepared in methanol. All stock solutions were stored at $-20^{\circ}C$.

Cell culture and induction of cell death

HeLa S3 cells were propagated at 37°C in a humidified atmosphere containing 5% CO_2 in DMEM/F12 medium supplemented with 10% FCS plus penicillin (100 μg/ml), streptomycin (100 U/ml), 4.5 mg/ml glucose, 50 μg/ml sodium pyruvate and 100 μg/ml uridine.

To deplete mitochondrial DNA (mtDNA), HeLa cells were grown during 2 months in the presence of 0.2 μg/ml ethidium bromide (EtB). Several sublines were isolated and checked for mtDNA depletion using a specific PCR. Two clones of HeLa cells lacking mtDNA (rho^0) were obtained (named clones B4 and B5). Cells lacking mtDNA were auxotrophic for uridine and pyruvate (King and Attardi, 1989). Therefore, both rho^0 and control cells were maintained in standard medium supplemented with pyruvate and uridine, The cultures were screened regularly for the absence of mycoplasma by a DNA-fluorochrome assay.

Cell death was induced by addition of TNF-α (5 ng/ml) plus emetine (1 μg/ml) on exponentially growing adherent cells. Cells treated with emetine alone or with TNF-α alone were used as controls.

Flow cytometric analysis

Mitochondrial membrane potential, ROS production and glutathione Mitochondrial membrane potential was assessed by the retention of $DiOC_6(3)$. The cationic lipophilic fluorochrome $DiOC_6(3)$ is a cell permeable marker that, at low doses (0.1 μM), specifically accumulates into mitochondria depending on mitochondrial membrane potential (Petit *et al*., 1990). ROS generation was measured by the production of dichlorofluorescein (DCF) derived from oxidization of DCFH. DCFH-DA is a fluorogenic freely permeable tracer specific for ROS assessment. DCFH-DA is deacetylated by intracellular esterases to the nonfluorescent compound DCFH, which is oxidized to the fluorescent compound DCF by a variety of peroxides, including hydrogen peroxide. Intracellular reduced glutathione (GSH) level was assessed using a specific probe, monobromobimane (mBBr). The cell permeant mBBr probe is non-fluorescent but forms a fluorescent adduct with GSH (GS-mBBr) in a nonenzymatic reaction. Plasma membrane integrity was examinated by PI exclusion from the cell compartment.

Cell stainings were performed as follows: cells were harvested at different time points of the emetine plus TNF-α (E/TNF) treatment, centrifuged and resuspended in complete medium at a concentration of 10^6 cells/ml. Cells were then loaded either with $DiOC_6(3)$ (0.1 μM), or DCFH-DA (20 μM) for 30 min or with mBBr (50 μM) for 10 min. Labellings were processed at 37°C in a humidified 5% CO_2/95% air incubator. Prior to flow cytometric analysis, all samples were incubated with PI (10 μg/ml) for 5 min at 4°C.

Flow cytometric measurements Flow cytometric measurements were performed on a ELITE ESP flow cytometer (Coulter®, France). Fluorescence excitation was obtained through the blue line (488 nm) of an argon ion laser operating at 15 mW. Green fluorescence of $DiOC_6(3)$ or DCF was collected with a 525 nm band pass filter and red fluorescence of PI with a 610 nm band pass filter. A 100 mW UV excitation (356 nm) from a Coherent laser (INOVA 305) was used for quantification of GS-mBBr fluorescence integrated above 457 nm. Analyses were performed on 10^4 cells and data were stored in listmode. Light scatter values were measured on a linear scale of 1024 channels and fluorescence intensities on a logarithmic scale of fluorescence of four decades of log.

In vivo *fluorescent measurement of ROS and mitochondrial transmembrane potential*

Cells were seeded on glass coverslips. E/TNF or emetine alone was added and at appropriate time points, cells were loaded with $DiOC_6(3)$ (0.1 μM) or DCFH-DA (20 μM) and DAPI (1 μg/ml) for 30 min at 37°C. DAPI was used to estimate the nuclear condensation. After loading, the coverslips were disposed on a slide chamber containing fresh medium without drug and cells were then immediately examined by epifluorescence and photographed under a DMRB Leica microscope.

Abbreviations

ΔΨm, mitochondrial membrane potential; BHA, butylated hydroxyanisole; DAPI, diamidino phenylindole; DCF, dichlorofluorescein; DCFH-DA, dichlorofluorescin diacetate; $DiOC_6(3)$, 3,3′-diethyloxacarbocyanine; E/TNF, emetine/TNF-α; EtB, ethidium bromide; FSC, forward angle scatter; GSH, glutathione; mBBr, monobromobimane; mtDNA, mitochondrial DNA; PCD, programmed cell death; PI, propidium iodide; ROS, reactive oxygen species; SSC, side angle scatter; TNF-α, tumor necrosis factor-α; Z-VAD, Z-Val-Ala-DL-Asp-fluoromethylketone.

Acknowledgements

We thank Drs Spencer Brown and Isabelle Guénal for their critical reading of the manuscript. This work was supported in part by grants from The Association pour la Recherche contre le Cancer (#6960) and from the Ministère de l'Education Nationale de l'Enseignement Supérieur et de la Recherche (ACC-SV4).

References

Beg AA and Baltimore D. (1996). *Science,* **274,** 782–784.

Beidler DR, Tewari M, Friesen PD, Poirier G and Dixit VM. (1995). *J. Biol. Chem.,* **270,** 16526–16528.

Bojes HK, Datta K, Xu J, Chin A, Simonian P, Nunez G and Kehrer JP. (1997). *Biochem. J.,* **325,** 315–319.

Boldin MP, Goncharov TM, Goltsev YV and Wallach D. (1996). *Cell,* **85,** 803–815.

Chinnaiyan AM, O'Rourke K, Lane BR and Dixit VM. (1997). *Science,* **275,** 1122–1126.

Chinnaiyan AM, O'Rourke K, Tewari M and Dixit VM. (1995). *Cell,* **8145,** 505–512.

Desjardins P, Frost E and Morais R. (1985). *Mol. Cell. Biol.,* **5,** 1163–1169.

Duan H, Chinnaiyan AM, Hudson PL, Wing JP, He WW and Dixit VM. (1996). *J. Biol. Chem.,* **271,** 1621–1625.

Ellerby LM, Ellerby HM, Park SM, Holleran AL, Murphy AN, Fiskum G, Kane DJ, Testa MP, Kayalar C and Bredesen DE. (1996). *J. Neurochem.,* **67,** 1259–1267.

Ellis RE, Yuan JY and Horvitz HR. (1991). *Annu. Rev. Cell Biol.,* **7,** 663–698.

France-Lanord V, Brugg B, Michel PP, Agid Y and Ruberg M. (1997). *J. Neurochem.,* **69,** 1612–1621.

Fraser A and Evan G. (1996). *Cell,* **85,** 781–784.

Gamen S, Anel A, Montoya J, Marzo I, Pineiro A and Naval J. (1995). *FEBS Lett.,* **376,** 15–18.

Golstein P. (1997). *Science,* **275,** 1081–1082.

Goossens V, Grooten J, De VK and Fiers W. (1995). *Proc. Natl. Acad. Sci. USA,* **92,** 8115–8119.

Greenlund LJS, Deckwerth TL and Johnson Jr EM. (1995). *Neuron,* **14,** 303–315.

Gudz TI, Tserng KY and Hoppel CL. (1997). *J. Biol. Chem.,* **272,** 24154 – 24158.
Higuchi M, Aggarwal BB and Yeh ET. (1997). *J. Clin. Invest.,* **99,** 1751 – 1758.
Hsu H, Xiong J and Goeddel DV. (1995). *Cell,* **8145,** 495 – 504.
Jacobson MD. (1996). *Trends Biochem. Sci.,* **21,** 83 – 86.
Jacobson MD and Raff MC. (1995). *Nature,* **374,** 814 – 816.
Kane DJ, Sarafian TA, Anton R, Hahn H, Gralla EB, Valentine JS, Ord T and Bredesen DE. (1993). *Science,* **262,** 1274 – 1277.
Kerr JFR, Wyllie AH and Currie AR. (1972). *Br. J. Cancer,* **26,** 239 – 257.
King MP and Attardi G. (1989). *Science,* **246,** 500 – 503.
Kluck RM, Bossy-Wetzel E, Green DR and Newmeyer DD. (1997). *Science,* **275,** 1132 – 1136.
Korsmeyer SJ. (1995). *Trends Genet.,* **11,** 101 – 105.
Krippner A, Matsuno-Yagi A, Gootlieb RA and Babior BM. (1996). *J. Biol. Chem.,* **271,** 21629 – 21636.
Kroemer G, Petit PX, Zamzami N, Vayssière JL and Mignotte B. (1995). *FASEB J.,* **9,** 1277 – 1287.
Kroemer G, Zamzami N and Susin SA. (1997). *Immunol. Today,* **18,** 44 – 51.
Liu X, Kim CN, Yang J, Jemmerson R and Wang X. (1996a). *Cell,* **86,** 147 – 157.
Liu ZG, Hsu H, Goeddel DV and Karin M. (1996b). *Cell,* **87,** 565 – 576.
Marchetti P, Decaudin D, Macho A, Zamzami N, Hirsch T, Susin SA and Kroemer G. (1997). *Eur. J. Immunol.,* **27,** 289 – 296.
Marchetti P, Susin SS, Decaudin D, Gamen S, Castedo M, Hirsch T, Zamzami N, Naval J, Senik A and Kroemer G. (1996). *Cancer Res.,* **56,** 2033 – 2038.
Martin DA, Siegel RM, Zheng L and Lenardo MJ. (1998). *J. Biol. Chem.,* **273,** 4345 – 4349.
Mayer M and Noble M. (1994). *Proc. Natl. Acad. Sci. USA,* **91,** 7496 – 500.
McCarthy NJ, Whyte MKB, Gilbert CS and Evan GI. (1997). *J. Cell Biol.,* **136,** 215 – 227.
Mehlen P, Schulze-Osthoff K and Arrigo AP. (1996). *J. Biol. Chem.,* **271,** 16510 – 16514.
Mignotte B and Vayssière JL. (1998). *Eur. J. Biochem.,* **252,** 1 – 15.
Minn AJ, Velez P, Schendel SL, Liang H, Muchmore SW, Fesik SW, Fill M and Thompson CB. (1997). *Nature,* **385,** 353 – 357.
Mirkovic N, Voehringer DW, Story MD, McConkey DJ, McDonnell TJ and Meyn RE. (1997). *Oncogene,* **15,** 1461 – 1470.
Miura M, Friedlander RM and Yuan J. (1995). *Proc. Natl. Acadl. Sci. USA,* **92,** 8318 – 8322.
Muchmore SW, Sattler M, Liang H, Meadows RP, Harlan IE, Yoon HS, Nettesheim D, Chang BS, Thompson CB, Wong SL, Ng SC and Fesik SW. (1996). *Nature,* **381,** 335 – 341.
Nagata S. (1997). *Cell,* **88,** 355 – 365.
O'Donnell VB, Spycher S and Azzi A. (1995). *Biochem. J.,* **310,** 133 – 141.
Packer MA and Murphy MP. (1994). *FEBS Lett.,* **345,** 237 – 240.
Petit PX, Lecoeur H, Zorn E, Dauguet C, Mignotte B and Gougeon ML. (1995). *J. Cell Biol.,* **130,** 157 – 167.
Petit PX, O'Connor J, Grunwald D and Brown SC. (1990). *Eur. J. Biochem.,* **194,** 389 – 397.
Quillet-Mary A, Jaffrezou JP, Mansat V, Bordier C, Naval J and Laurent G. (1997). *J. Biol. Chem.,* **272,** 21388 – 21395.
Raff MC. (1992). *Nature,* **356,** 397 – 400.
Reed JC. (1997). *Nature,* **387,** 773 – 776.
Sandstrom PA and Buttke TM. (1993). *Proc. Natl. Acad. Sci. USA,* **90,** 4708 – 4712.
Sato N, Iwata S, Nakamura K, Hori T, Mori K and Yodoi J. (1995). *J. Immunol.,* **154,** 3194 – 3203.
Scaffidi C, Fulda S, Srinivasan A, Friesen C, Li F, Tomaselli PU, Debatin KM, Krammer PH and Peter ME. (1998). *EMBO J.,* **17,** 1675 – 1687.
Schendel SL, Xie Z, Montal MO, Matsuyama S, Montal M and Reed JC. (1997). *Proc. Natl. Acad. Sci. USA,* **94,** 5113 – 5118.
Schulze-Osthoff K, Bakker AC, Vanhaesebroeck B, Beyaert R, Jacob WA and Fiers W. (1992). *J. Biol. Chem.,* **267,** 5317 – 5323.
Schulze-Osthoff K, Beyaert R, Vandevoorde V, Haegeman G and Fiers W. (1993). *EMBO J.,* **12,** 3095 – 3104.
Schulze-Osthoff K, Krammer PH and Droge W. (1994). *EMBO J.,* **13,** 4587 – 4596.
Shaham S and Horvitz HR. (1996). *Genes Dev.,* **10,** 578 – 591.
Shimizu S, Eguchi Y, Kosaka H, Kamiike W, Matsuda H and Tsujimoto Y. (1995). *Nature,* **374,** 811 – 813.
Stanger BZ, Leder P, Lee T, Kim E and Seed B. (1995). *Cell,* **811,** 513 – 523.
Susin SA, Zamzani N, Castedo M, Hirsh T, Marchetti P, Macho A, Daugas E, Geuskens M and Kroemer G. (1996). *J. Exp. Med.,* **184,** 1 – 11.
Talley AK, Dewhurst S, Perry SW, Dopllard SC, Gummuluru S, Fine SM, New D, Epstein LG, Gendelman HE and Gelbard HA. (1995). *Mol. Cell. Biol.,* **15,** 2359 – 2366.
Van Antwerp DJ, Martin SJ, Kafri T, Green DR and Verma IM. (1996). *Science,* **274,** 787 – 789.
van den Dobbelsteen DJ, Nobel CSI, Schlegel J, Cotgreave IA, Orrenius S and Slater AFG. (1996). *J. Biol. Chem.,* **271,** 15420 – 15427.
Vayssière JL, Petit PX, Risler Y and Mignotte B. (1994). *Proc. Natl. Acad. Sci. USA,* **91,** 11752 – 11756.
Wang CY, Mayo MW and Baldwin Jr. AS. (1996). *Science,* **274,** 784 – 787.
Weil M, Jacobson MD, Coles HSR, Davies TJ, Gardner RL, Raff KD and Raff MC. (1996). *J. Cell Biol.,* **133,** 1053 – 1059.
Wong GHW, Elwell JH, Oberley LW and Goeddel DV. (1989). *Cell,* **58,** 923 – 931.
Wu D, Wallen HD and Nunez G. (1997). *Science,* **275,** 1126 – 1129.
Yang J, Liu X, Bhalla K, Kim CN, Ibrado AM, Cai J, Peng TI, Jones DP and Wang X. (1997). *Science,* **275,** 1129 – 1132.
Yuan JY, Shaham S, Ledoux S, Ellis HM and Horvitz HR. (1993). *Cell,* **75,** 641 – 652.
Zamzami N, Marchetti P, Castedo M, Zanin C, Vayssière JL, Petit PX and Kroemer G. (1995). *J. Exp. Med.,* **181,** 1661 – 1672.
Zamzami N, Susin SA, Marchetti P, Hirsch T, Gomez-Monterrey I, Castedo M and Kroemer G. (1996). *J. Exp. Med.,* **183,** 1533 – 1544.